GEOSCIENCE FRONTIERS 2(3) (2011) 439–447

available at www.sciencedirect.com

China University of Geosciences (Beijing)

GEOSCIENCE FRONTIERS

journal homepage: www.elsevier.com/locate/gsf

ORIGINAL ARTICLE

Effects of hydrocarbon generation on fluid flow in the Ordos Basin and its relationship to uranium mineralization

Chunji Xue [a,b,*], **Guoxiang Chi** [c], **Wei Xue** [b]

[a] *State Key Laboratory of Geological Processes and Mineral Resources, China University of Geosciences, Beijing 100083, China*
[b] *School of the Earth Sciences and Resources, China University of Geosciences, Beijing 100083, China*
[c] *Department of Geology, University of Regina, Regina, Saskatchewan, Canada*

Received 6 January 2011; accepted 24 March 2011
Available online 17 June 2011

KEYWORDS
Ordos Basin;
Uranium deposits;
Hydrodynamics;
Hydrocarbon generation;
Fluid overpressure;
Fluid flow;
Numerical modeling

Abstract The Ordos Basin of North China is not only an important uranium mineralization province, but also a major producer of oil, gas and coal in China. The genetic relationship between uranium mineralization and hydrocarbons has been recognized by a number of previous studies, but it has not been well understood in terms of the hydrodynamics of basin fluid flow. We have demonstrated in a previous study that the preferential localization of Cretaceous uranium mineralization in the upper part of the Ordos Jurassic section may have been related to the interface between an upward flowing, reducing fluid and a downward flowing, oxidizing fluid. This interface may have been controlled by the interplay between fluid overpressure related to disequilibrium sediment compaction and which drove the upward flow, and topographic relief, which drove the downward flow. In this study, we carried out numerical modeling for the contribution of oil and gas generation to the development of fluid overpressure, in addition to sediment compaction and heating. Our results indicate that when hydrocarbon generation is taken into account, fluid overpressure during the Cretaceous was more than doubled in comparison with the simulation when hydrocarbon generation was not considered. Furthermore, fluid overpressure dissipation at

* Corresponding author. State Key Laboratory of Geological Processes and Mineral Resources, China University of Geosciences, Beijing 100083, China.
E-mail address: chunji.xue@cugb.edu.cn (C. Xue).

Peer-review under responsibility of China University of Geosciences (Beijing).
doi:10.1016/j.gsf.2011.05.007

the end of sedimentation slowed down relative to the no-hydrocarbon generation case. These results suggest that hydrocarbon generation may have played an important role in uranium mineralization, not only in providing reducing agents required for the mineralization, but also in contributing to the driving force to maintain the upward flow.

1. Introduction

The Ordos Basin in northern China is an emerging uranium mineralization province, and is also one of the top oil, gas and coal producers in China (Wei and Wang, 2004; Chen et al., 2005; Deng et al., 2005). The potential relationship between uranium mineralization and organic matter or oil and gas in the Ordos Basin has been recognized by a number of previous studies (e.g., Zhang, 2004; Feng et al., 2006; Peng et al., 2007; Xue et al., 2009), and it has been generally agreed that uranium mineralization took place where oxidizing, uranium-carrying fluids met reducing agents (Xiao et al., 2004; Chen et al., 2006). The location where the two fluids met was likely controlled by the hydrodynamic regime of the basin, which has received relatively little attention until recently.

Xue et al. (2010) carried out numerical modeling of Ordos basinal fluid flow, taking into consideration the effects of disequilibrium sediment compaction and topographic relief. Based on their modeling results, they proposed that two fluid flow systems were developed in Jurassic and Cretaceous time when the margins of the basin were relatively uplifted and the strata within it were gently inclined. An upper fluid flow system was driven by gravity in relation to topographic relief and the flow direction was downward from the basin margin to its center. A lower flow system, driven by overpressures related to sediment compaction, was upward from the basin center toward its margins (Xue et al., 2010). It was further proposed that the location of the interface between the two fluid systems, where oxidizing, uranium-carrying fluid reacted with reducing, hydrocarbons-bearing fluid and uranium ore minerals were precipitated, was a function of the magnitudes of the two competing driving forces, i.e., compaction-driven versus topography-driven flows (Xue et al., 2010). Because the fluid overpressure caused by disequilibrium sediment compaction was fairly small (about 20 bar), the location of the interface between the two fluid systems was strongly influenced by topographic relief (Xue et al., 2010).

Many studies have suggested that hydrocarbon generation can be a major contribution to the development of overpressures in sedimentary basins (Bredehoeft et al., 1994; Luo and Vasseur, 1996; Lee and Williams, 2000; McPherson and Bredehoeft, 2001; Hansom and Lee, 2005). In order to further understand the localization of uranium mineralization in the Ordos basin, this study extends the numerical modeling of Xue et al. (2010) by taking into account the effect of oil and gas generation on fluid overpressure development, in addition to the effects of disequilibrium sediment compaction. We simulated the evolution of fluid overpressure, fluid flow rate and temperature in a representative cross section of the Ordos Basin for situations with and without hydrocarbon generation. The results of the two situations are compared to evaluate how hydrocarbon generation may have influenced Ordos basinal fluid flow patterns and the localization of uranium mineralization.

2. Geologic setting

The Ordos Basin is located on the North China craton, between the Hercynian Inner Mongolia–Daxinganling orogen to the north and the Indo-Sinian Qilian–Qinling orogen to the south (Fig. 1A, B). It is bordered by the Alashan block on the west and by the Shanxi block on the east (Fig. 1B). The basin was developed during the Mesozoic on an upper basement of Paleozoic sedimentary rocks, which are underlain by Precambrian crystalline basement rocks. Because hydrocarbon reservoirs are found in both the Paleozoic and Mesozoic rocks (Deng et al., 2005), the Paleozoic strata are generally treated as part of the Ordos Basin rather than basement (Fig. 1C).

The Paleozoic section consists of Cambrian and Ordovician marine carbonates and mud rocks, a hiatus from Silurian to Devonian, marginal marine, coal-bearing sediments of Carboniferous age, and fluvial — lacustrine coal-bearing formations of Permian age. From the Triassic to Cretaceous, the Ordos Basin was filled with fluvial and lacustrine sediments — mostly sandstones and shales. Triassic strata consist of the Liujiagou, Heshanggou, Zifang and Yanchang formations in ascending order. The Jurassic rocks are separated from the Triassic by an unconformity, and include (from oldest to youngest) the Fuxian, Yan'an, Zhiluo, Anding and Fenfang formations. Cretaceous strata unconformably overlie the Jurassic rocks and consist of the Yijun, Luohe, Huachi, Luohandong and Jinchuan formations. The entire basin was uplifted after the late Cretaceous, forming a series of smaller grabens and horsts (Chen et al., 2005; Deng et al., 2005). Overall the basin was characterized by uplifting in the east and relative subsidence in the west during the Mesozoic time (Deng et al., 2005).

The Ordos Basin is different from typical craton basins in that basin margins were tectonically active, whereas the interior of the basin was relatively stable. The strata in the interior of the basin are generally horizontal or gently dipping (1°–3°), whereas those in the marginal parts of the basin were subjected to significant folding and faulting during Yanshanian (Jurassic and Cretaceous) orogeny.

Hydrocarbon source rocks have been found in Upper and Lower Paleozoic strata, and large-scale gas generation has been estimated to have occurred in the Jurassic and Cretaceous (Ren, 1996). A number of uranium deposits and occurrences have been found along the margins of the Ordos Basin. They are concentrated in the Dongsheng-Zhungerqi area in the northeast, the Suide-Mizhi and Yanchang-Yanchuan areas in the east, the Huangling-Binxian and Hancheng-Baishui areas in the southeast, the Longxian-Pingliang area in the southwest, the Ciyaobao-Shigouyi area in the west, and the Ertuokeqi area in the north (Fig. 1A). The most important uranium deposits include Shengshangou in Dongsheng, Guojiawan in Longxian, and Diantou in Huangling (Xue et al., 2010). Except for minor occurrences in carbonaceous shales, most uranium mineralization occurs in

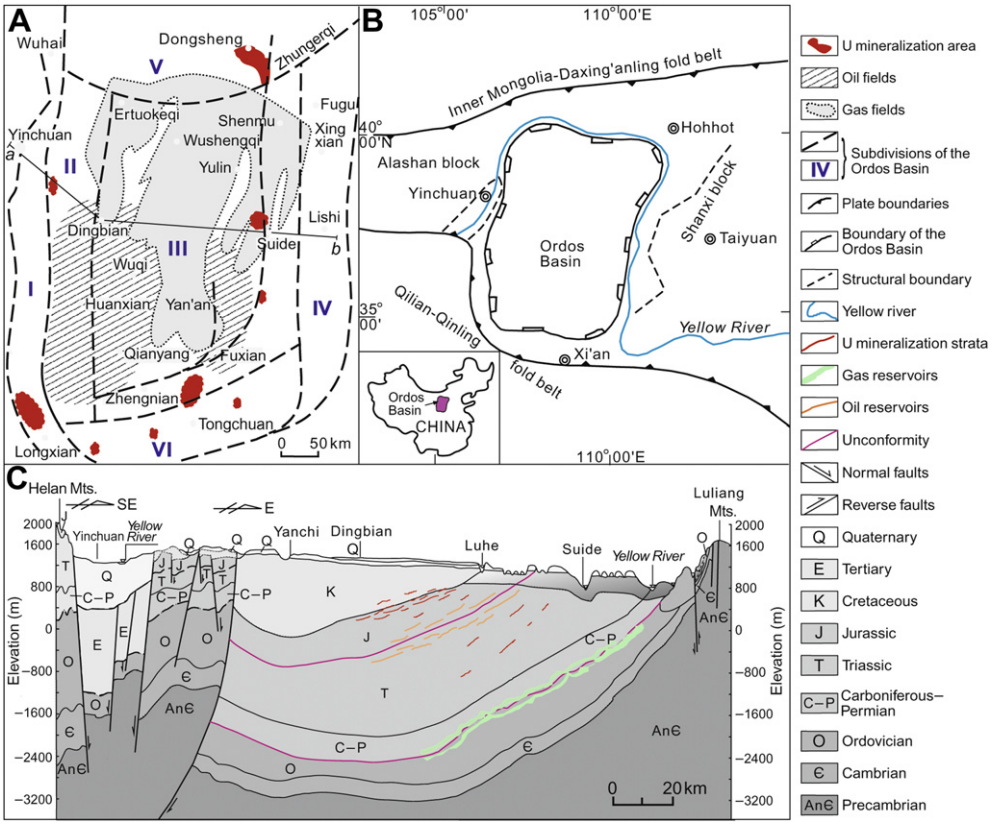

Figure 1 A) Distribution of oil, gas and uranium mineralization in the Ordos Basin. Subdivisions of the basin include the Western Margin Thrust-Faulting Belt (I), Western Depression Belt (II), Eastern Slope Belt (III), Western Shanxi Fold Belt (IV), Yi-Meng Uplift (V), and Weibei Uplift (VI). Line *a*–*b* indicates the approximate location of the cross section shown in Fig. 1C. B) Regional tectonic setting of the Ordos Basin. The location of the Ordos Basin in China is shown in the insert. C) A conceptual west-east cross section of the Ordos Basin, showing the major strata of oil and gas accumulations and uranium mineralization (after Wang et al., 2004).

sandstones. Orebodies are typically tabular. The host strata include the Triassic Liujiagou, Heshanggou, Zhifang and Yanchang formations, the Jurassic Yan'an, Zhiluo and Anding formations, and the Cretaceous Huachi and Jinchuan formations, the most important of these being the Zhiluo Formation.

Although the deposits are located only a few hundred meters below the modern surface, geologic, petrographic and fluid inclusion studies suggest that the uranium mineralization took place at temperatures from 60 to 180 °C (Li et al., 2006; Ling, 2007), which indicates either deep-burial or hydrothermal, rather than early diagenetic environments (Xue et al., 2010). The ages of uranium mineralization (U–Pb isochron method) in the Dongsheng area fall in a wide range, including 177–149, 124–107, 85–74 and 20–8 Ma, with the Late Cretaceous interval being the most important (Xia et al., 2003; Liu et al., 2007). Two U–Pb isochron ages of the Diantou uranium deposit are 51 and 42 Ma (Chen et al., 2006).

3. Conceptual model and study methods

This study's numerical modeling is based on a conceptual cross section of the Ordos Basin in a west–east direction (Fig. 1C), as also used in Xue et al. (2010). The model cross section is divided into six hydrostratigraphic units, i.e., Cambrian, Ordovician, Carboniferous–Permian, Triassic, Jurassic, and Cretaceous, with a hiatus between the Ordovician and Carboniferous and another between the Triassic and Jurassic (Table 1). The basin center is chosen at the thickest section of the Cretaceous sediments, and the basin margin is set near Luliangshan (Fig. 1C). An additional 1340 m of Cretaceous sediments was added on top of the section in Fig. 1C to account for erosion (Ren et al., 2006). The lithology, time interval, total organic carbon (TOC), and thickness (m) of the different hydrostratigraphic units used in the numerical model are listed in Table 1. The hiatuses are represented by only 1 m of sediments over a long period of time.

The model is closed to fluid flow on the left (west) and bottom and open on the right (east) and surface. A heat flux of 59.55 mW/m^2 is supplied from the bottom based on an estimation of geothermal gradient of 3.1 °C/100 m (Ren et al., 2006), and a fixed temperature of 20 °C is set on the surface. The fluid properties (thermal expansion coefficient, compressibility coefficient, heat capacity, and heat conductivity), solid matrix properties (density, heat capacity, and heat conductivity), and parameters related to porosity as a function of depth and permeability as a function of porosity, are generic and are adopted from Bethke (1985) and Garven (1985), as summarized by Chi and Savard (1998) and Chi et al. (2010). Hydrocarbon properties and kinematic parameters (including kerogen-to-oil conversion and oil-to-gas conversion) used in the modeling are based on type-II kerogens as the dominant hydrocarbon generator (Yang and Pei, 1996; He, 2003; Li et al., 2005), and are adopted from Lee and Williams

Table 1 Lithology, time interval, TOC, and thickness (m) of hydrostratigraphic units of the Ordos Basin*.

Unit	Lithology**	Time interval	TOC***	Thickness (m)												
		(Ma)	(wt. %)	0	1	2	3	4	5	6	7	8	9	10	11	12	13	14
Distance from basin center				0	10	20	30	40	50	60	70	80	90	100	110	120	130	140
K	40% sd + 5% lms + 55% sh	145 – 65	1.00	3000	2900	2800	2700	2600	2500	2400	2300	2200	2100	2000	1900	1800	1700	1600
J	50% sd + 5% lms + 45% sh	200 – 145	2.05	583	591	724	770	705	674	585	555	538	521	469	427	384	341	299
Hiatus	30% sd + 5% lms + 65% sh	205 – 200	0.00	1	1	1	1	1	1	1	1	1	1	1	1	1	1	1
T	30% sd + 5% lms + 65% sh	245 – 205	2.12	1086	1284	1459	1580	1680	1690	1563	1482	1521	1435	1280	1109	939	768	597
C–P	20% sd + 5% lms + 75% sh	360 – 245	1.77	561	550	504	493	472	495	308	410	429	421	478	370	306	247	188
Hiatus	95% lms + 5% sh	440 – 360	0.00	1	1	1	1	1	1	1	1	1	1	1	1	1	1	1
O	95% lms + 5% sh	520 – 440	0.23	524	316	312	378	469	561	735	731	747	696	671	494	381	265	145
Cam	95% lms + 5% sh	556 – 520	0.14	317	329	329	322	329	322	285	300	303	271	270	232	214	172	128

*Modified from Xue et al. (2010).
**sd = sandstone; sh = shale; lms = limestone.
***TOC contents are based on compilation of data from Dai (1997), Li et al. (2005), Yang and Pei (1996), Mou (2001), Sun (2005), and Xue et al. (2009).

(2000), Speight (2006), Pepper and Corvi (1995) and Pepper and Dodd (1995) as summarized in Chi et al. (2010).

In the study by Xue et al. (2010), the program Basin2™ (Bethke et al., 1993) was used. Because Basin2 does not have a module of hydrocarbon generation we used the program BsnMod in the present study. It was initially developed by Chi and Savard (1998) and Chi (2001) based on the mathematical model of Bethke (1985), with a module of hydrocarbon generation being added by Chi et al. (2010). Detailed derivation and description of the governing equations (medium continuity, mass balance, energy conservation, and hydrocarbon generation) can be found in Bethke (1985) and Chi et al. (2010), and are not repeated here. The use of the program BsnMod is briefly described as follows.

The main interface of BsnMod (Fig. 2A) shows all the input buttons including model selection, basin data, fluid properties, solid properties, porosity–permeability parameters, boundary conditions, numerical parameters, and parameters related to hydrocarbon generations. Among all the inputs, the "basin data" table (Fig. 2B) is the most complex, which contains all the data from Table 1. The other tables (e.g., Fig. 2C, D, E and F) are mostly of default values adopted from sources as discussed above. In the menu and tool bar in Fig. 2A, there are two output functions; one is for graphical output and the other for spreadsheet output. The graphical output contains the calculation grids, fluid flow vectors, contours of fluid overpressure and contours of temperature, which can be copied to other graphical software such as CorelDraw for further editing. The spreadsheet output contains all the calculation results for each node of the grid — including coordinates, temperature, fluid pressure, fluid overpressure, fluid flow velocity, porosity, permeability, fraction of oil generation, and fraction of gas generation, which can be copied to other program such as Excel for further data manipulation.

4. Simulation results

The evolution of fluid flow rate, fluid pressure, fluid overpressure, and temperature was simulated for the Ordos Basin through time from the Cambrian to the Tertiary. Two sets of simulation were carried out — one considering the effect of disequilibrium sediment compaction and temperature on fluid overpressure and fluid flow, and the other considering oil and gas generation in addition to the first set parameters. The simulation of the effects of topography, which had been done by Xue et al. (2010), was not carried out in this study.

Simulation results without considering hydrocarbon generation are shown in Fig. 3. Fluid overpressures were negligible during the deposition of the Cambrian and Ordovician sediments, with the maximum overpressure contour being only 0.04 bar. The maximum fluid overpressure contour value increased to 10.8 bar by the end of the Triassic (205 Ma), decreased to 5.6 bar by the end of the Jurassic (145 Ma), increased again to 22.2 bar by the end of the Cretaceous (65 Ma), and then decreased to 8.1 bar at 20 Ma. Throughout the history of the basin, fluid flow was mainly upward and toward the basin margin (right side of the model, Fig. 3, left column). Locally downward fluid flow was developed due to fluid overpressure being lower in the Cambrian and Ordovician strata than in the overlying Carboniferous, Permian and Triassic strata. Fluid flow velocities were generally very slow, with the maximum horizontal flow rate being 0.137 cm/year and maximum vertical flow rate being

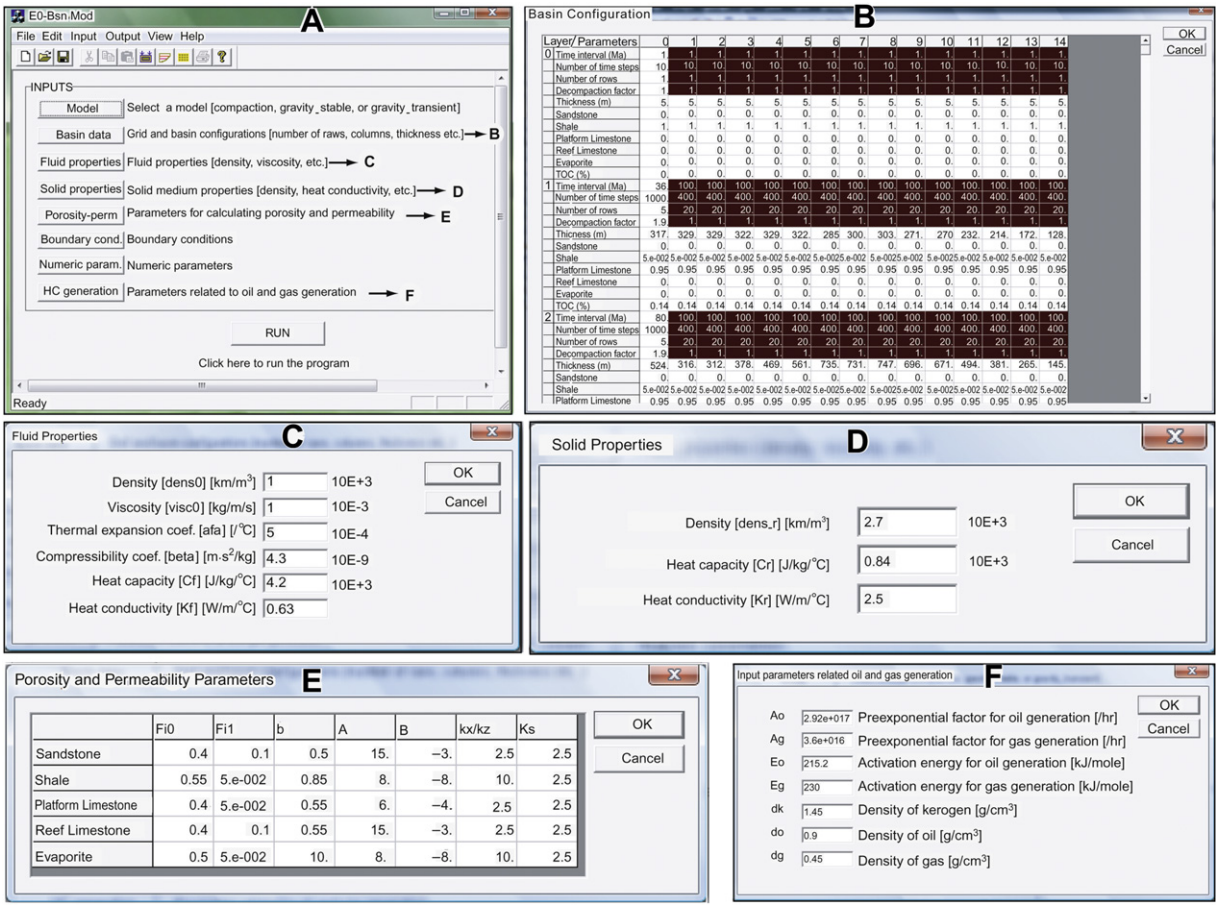

Figure 2 User interfaces of the BsnMod program. A) Main interface showing various input and output buttons; B) input of basin data; C) input of fluid properties; D) input of solid properties; E) input of porosity and permeability parameters; F) input of parameters related to oil and gas generation.

0.00728 cm/year (Fig. 3). Corresponding to these small flow rates, the geothermal profile was almost non-disturbed, with the isotherms being almost horizontal (right column, Fig. 3). These simulation results are similar to those obtained by using Basin2 (Fig. 5 of Xue et al., 2010).

In the second simulation set, in which the effect of hydrocarbon generation was taken into account in the calculation of fluid overpressure, the fractions of oil and gas generated were computed and added to the parameters used in the first set of simulation. The results indicate that oil generation began in the Triassic in the lower part of the basin, and gradually moved upward during Jurassic and Cretaceous time; gas generation did not start until Cretaceous time and continued to evolve afterward. Fig. 4 is a "snapshot" of the oil and gas generation zones at the end of the Cretaceous time. The simulation results of fluid flow velocity, fluid overpressure and temperature from Cambrian to the end of Jurassic (145 Ma and before; Fig. 5) are almost identical to those without considering hydrocarbon generation (Fig. 3). This suggests that hydrocarbon generation was minor and made negligible contribution to fluid overpressure development during this period of time. However, by the end of Cretaceous, fluid overpressure (maximum fluid overpressure contour value = 59 bar, Fig. 5) was significantly higher than in the case of no-hydrocarbon generation (maximum fluid overpressure contour value = 22.2 bar, Fig. 3). By the time of 20 Ma, fluid overpressure with hydrocarbon generation (maximum fluid overpressure contour value = 18 bar, Fig. 5) was still much higher than the no-hydrocarbon generation counterpart (maximum fluid overpressure contour value = 8.1 bar, Fig. 3).

However, despite the prominent fluid overpressure patterns shown in Figs. 3 and 5, the magnitudes of fluid overpressure are actually fairly small, as illustrated by the depth–pressure profile of the basin center (Fig. 6). Without hydrocarbon generation, the fluid pressure at different depths of the basin was close to hydrostatic values throughout the basin history (Fig. 6A). With hydrocarbon generation, however, an increase of fluid pressure above the hydrostatic line is noticeable by the end of Cretaceous (65 Ma), which gradually dissipated and became almost indiscernible by 20 Ma (Fig. 6B).

5. Discussion and conclusions

As shown in Fig. 1C, the majority of uranium mineralization of the Ordos Basin is located in the upper part of the Jurassic section. According to the mixing model of uranium mineralization, this preferentially mineralized interval may have coincided with the interface between the reducing, upward flowing fluid system and

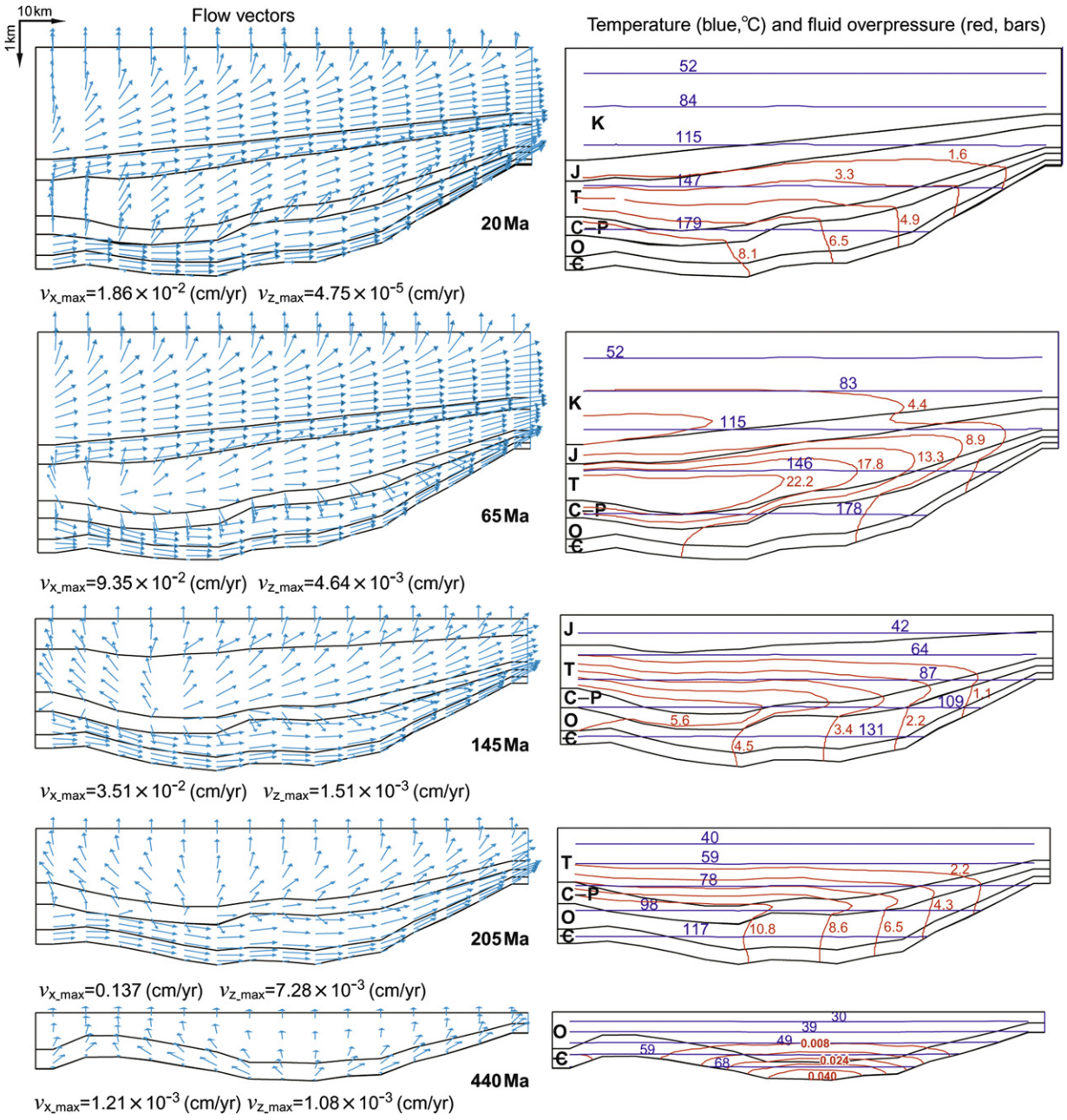

Figure 3 Numerical modeling results for simulations without considering hydrocarbon generation, showing fluid flow patterns, fluid overpressures, and isotherms at the end of Ordovician (440 Ma), end of Triassic (205 Ma), end of Jurassic (145 Ma), end of Cretaceous (65 Ma), and after ceasing of sedimentation (20 Ma).

the oxidizing, downward flowing fluid system (Xue et al., 2010). The accumulation of large amounts of uranium requires that this interface was relatively stable over a prolonged period of time.

From the ages of uranium mineralization, which range from 177 Ma to 8 Ma (Xia et al., 2003; Chen et al., 2006; Liu et al., 2007), it appears that uranium mineralization in the Ordos Basin may have started in early diagenetic stages of the Jurassic strata, but most likely continued after the Cretaceous. Although fluid overpressures were small during the history of the Ordos Basin based on numerical modeling results (this study and Xue et al., 2010), it has been shown that they were sufficient to maintain the upward fluid flow in the lower part of the basin against the downward forcing of the topography-driven fluid. The interface between the two fluid systems may have been located in the upper part of the Jurassic strata if the topographic relief was moderate (350 m across the model cross section). Because fluid overpressure dissipated gradually after the end of sedimentation, an accompanying decrease in topographic relief is required in order to maintain the interface between upward and downward flow systems at a relatively stable stratigraphic interval.

If the topographic relief did not reduce as much as the effect of overpressure dissipation, the downward flowing oxidizing fluid system would move deeper into the basin, leaching or remobilizing uranium minerals previously accumulated in the upper part

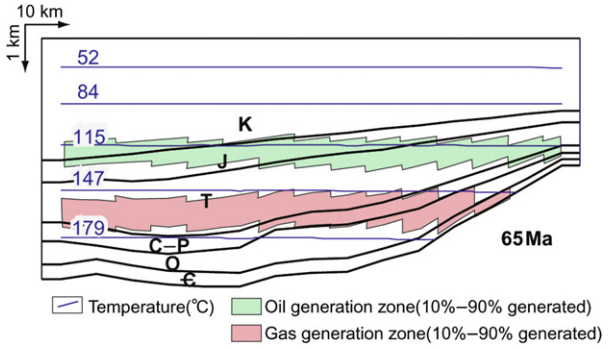

Figure 4 Numerical modeling results showing the distribution of oil generation (10%–90% oil generated) and gas generation (10%–90% gas generated) zones at the end of the Cretaceous (65 Ma).

of the basin (especially in the Jurassic). The results of the present study indicate that fluid overpressures were significantly increased, and the dissipation of fluid overpressure after the cessation of sedimentation slowed down, when the effect of hydrocarbon generation is considered (Fig. 5).

In conclusion, previous numerical modeling results indicate that two competing fluid flow systems, an upward flowing, reducing fluid and a downward flowing, oxidizing fluid, may have developed in the Ordos Basin during Jurassic and Cretaceous time. The stability of the interface between the two fluid systems, which is critical for uranium mineralization, was vulnerable to topographic change, especially after the ceasing of sedimentation. The fluid overpressure, which drives upward fluid flow, could have been significantly increased by oil and gas generation within the basin. If so, it may have played an important role in determining the location of the interface between the two fluid flow systems and, thus, constraining the localization of uranium mineralization.

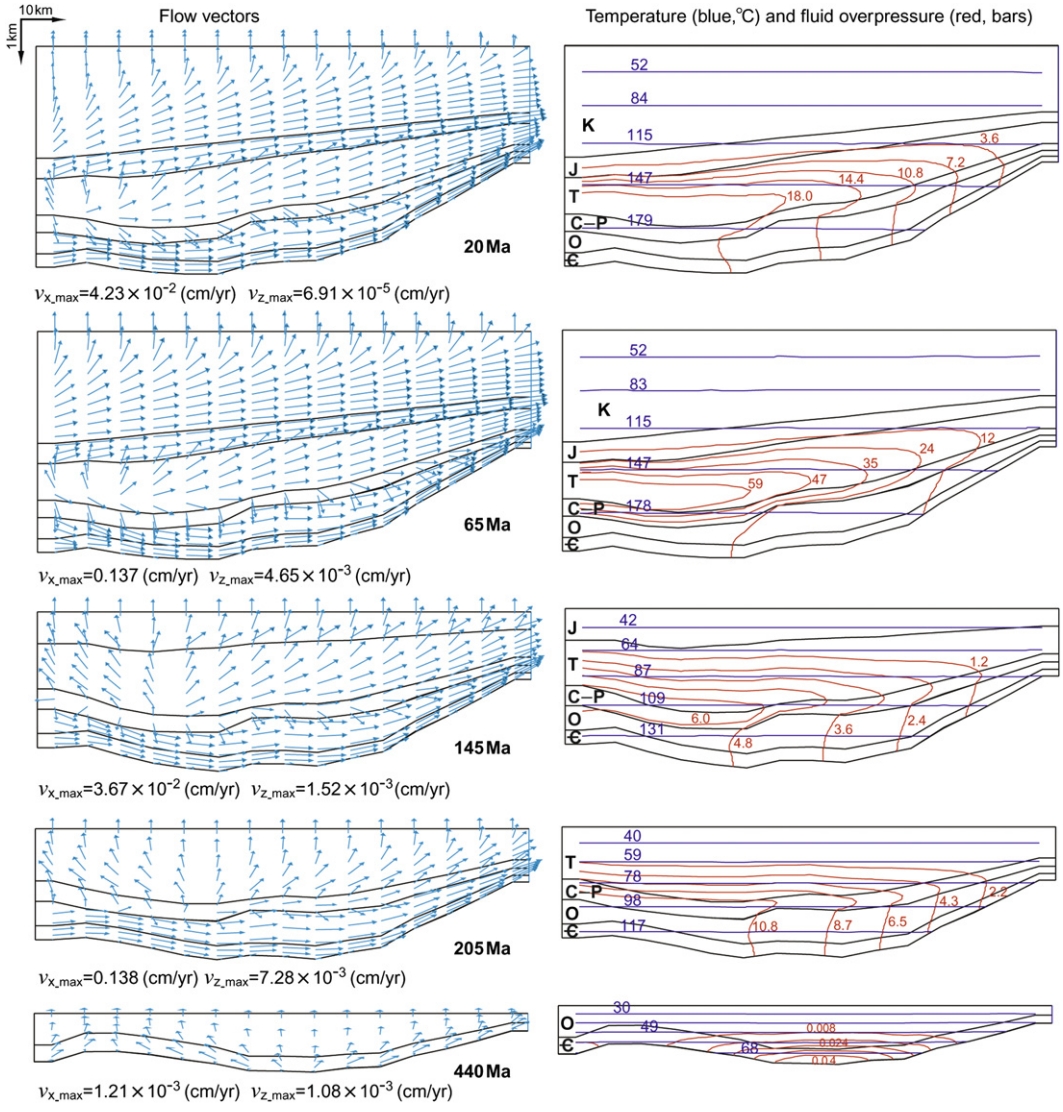

Figure 5 Numerical modeling results for simulations taking into account the contribution of hydrocarbon generation to overpressure development, showing fluid flow patterns, fluid overpressures, and isotherms at the end of Ordovician (440 Ma), end of Triassic (205 Ma), end of Jurassic (145 Ma), end of Cretaceous (65 Ma), and after the cessation of sedimentation (20 Ma).

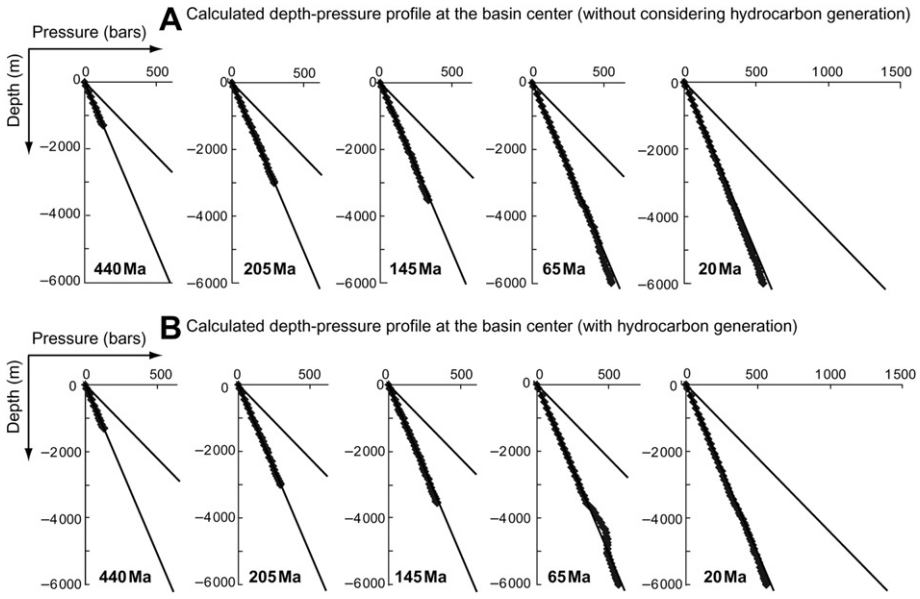

Figure 6 Calculated depth–pressure profile at the basin center (left side of the model) at various stages of the Ordos Basin for simulations without considering hydrocarbon generation (A) and with hydrocarbon generation (B). Note fluid pressure is close to hydrostatic values in most cases, but a prominent fluid pressure increase above the hydrostatic line is noticeable at 65 Ma when hydrocarbon generation is included in the simulation.

Acknowledgments

This study was supported by NSFC (41072069, 40772061 and 40930423), State Basic Research Plan (2009CB421005), IRT (0755) and 111 Plan (B07011) grants to Xue and an NSERC-Discovery grant to Chi. We would like to thank Jihu Cao for assistance in the compilation of data about the Ordos Basin, especially the TOC values and kerogen types.

References

Bethke, C.M., 1985. A numerical model of compaction-driven groundwater flow and heat transfer and its application to paleohydrology of intracratonic sedimentary basins. Journal of Geophysical Research 90, 6817–6828.

Bethke, C.M., Lee, M.-K., Quinodoz, H., Kreiling, W.N., 1993. Basin Modeling with Basin2, a Guide to Using the Basin2, B2plot, B2video, and B2view. University of Illinois, Urbana, p. 225.

Bredehoeft, J.D., Wesley, J.B., Fouch, T.D., 1994. Simulations of the origin of fluid pressure, fracture generation, and the movement of fluids in the Uinta Basin, Utah. AAPG Bulletin 78, 1729–1747.

Chen, G., Li, X., Zhou, L., 2005. Coupled relationships between tectonics and multiple mineralizations in the Ordos Basin. Earth Science Frontiers 12, 535–541 (in Chinese with English abstract).

Chen, H., Xu, G., Wang, J., Li, W., Zhao, X., 2006. Mineralization characteristics of the Diantou uranium deposit in the southern margin of Ordos and in comparison with the Dongsheng uranium deposit. Acta Geologica Sinica 80, 724–733 (in Chinese with English abstract).

Chi, G.X., 2001. BsnMod: A Windows Program for Simulating Basin-scale Fluid Flow and Heat Transfer Processes Related to Sediment Compaction and Tectonic Uplifting in Two Dimensions. Geological Survey of Canada, Current Research 2001, D-24, p. 7.

Chi, G.X., Lavoie, D., Bertrand, R., Lee, M.K., 2010. Downward hydrocarbon migration predicted from numerical modeling of fluid overpressure in the Paleozoic Anticosti Basin, eastern Canada. Geofluids 10, 334–350.

Chi, G.X., Savard, M.M., 1998. Basinal fluid flow models related to Zn-Pb mineralization in the southern margin of the Maritimes Basin, eastern Canada. Economic Geology 93, 896–910.

Dai, J.X., 1997. Natural Gas Accumulation Zones in China. Science Press, Beijing, p. 63.

Deng, J., Wang, Q.F., Gao, B.F., Huang, D.H., Yang, L.Q., Xu, H., Zhou, Y.H., 2005. Evolution of the Ordos Basin and its distribution of various energy and mineral resources. Geoscience 19 (4), 538–545 (in Chinese with English abstract).

Feng, J., Zhang, X., Wang, Y., Fan, A., Liu, Y., 2006. Migration and accumulation of hydrocarbons in Upper Paleozoic strata and their roles in uranium mineralization in the northern part of the Ordos Basin. Acta Geologica Sinica 80, 748–752 (in Chinese with English abstract).

Garven, G., 1985. The role of regional fluid flow in the genesis of the Pine Point deposit, Western Canada sedimentary basin. Economic Geology 80, 307–324.

Hansom, J., Lee, M.K., 2005. Effects of hydrocarbon generation, basal heat flow and sediment compaction on overpressure development: a numerical study. Petroleum Geoscience 11, 353–360.

He, Z.X., 2003. The Evolution of the Ordos Basin and Its Relationship with Oil and Gas. Petroleum Industry Press, p. 390 (in Chinese).

Lee, M.K., Williams, D.D., 2000. Paleohydrogeology of the Delaware Basin, western Texas: overpressure development, hydrocarbon migration, and ore genesis. AAPG Bulletin 84, 961–974.

Li, Q.X., Hou, D.J., Hu, G.Y., Li, J., 2005. Characteristics of Basinal Fluids and Formation of Natural Gas Reservoirs in the Central Part of the Ordos Basin. Geology Press, Beijing, p. 19 (in Chinese).

Li, R., He, Y., Li, J., Li, J., Li, X., 2006. Isotopic composition of fluid inclusions and origins of ore-forming fluids in the Dongsheng uranium deposit. Acta Geologica Sinica 80, 753–760.

Ling, M., 2007. Mineralogical and geochemical studies of sandstone-type uranium mineral deposits in the Ordos Basin. Ph.D. thesis, China University of Science and Technology, Hefei, p. 112 (in Chinese with English abstract).

Liu, H., Xia, Y., Tian, S., 2007. Geochronological and source studies of uranium mineralization in Dongsheng. Uranium Geology 23, 23–29 (in Chinese with English abstract).

Luo, X.R., Vasseur, G., 1996. Geopressuring mechanism of organic matter cracking: numerical modeling. AAPG Bulletin 80, 856–874.

McPherson, B.J.O.L., Bredehoeft, J.D., 2001. Overpressures in the Uinta basin, Utah: analysis using a three-dimensional basin evolution model. Water Resources Research 37, 857–871.

Mou, Z.H., 2001. Characteristics of the Mesozoic Oil-generation System in the Southern Part of the Ordos Basin. Petroleum Industry Press, Beijing, p. 93 (in Chinese).

Peng, Y., Chen, A., Fang, X., 2007. Relationships between hydrocarbons and the Dongsheng sandstone-type uranium deposit. Geochemistry 36, 267–274.

Pepper, A.S., Corvi, P.J., 1995. Simple kinetic models of petroleum formation. Part I: oil and gas generation from kerogen. Marine and Petroleum Geology 12, 291–319.

Pepper, A.S., Dodd, T.A., 1995. Simple kinetic models of petroleum formation. Part II: oil-gas cracking. Marine and Petroleum Geology 12, 321–340.

Ren, Z., 1996. Thermal history of the Ordos Basin and its relationship to oil and gas generation. Acta Petrolei Sinica 17, 17–24 (in Chinese with English abstract).

Ren, Z., Zhang, S., Gao, S., Cui, J., Liu, X., 2006. Relationship between thermal evolution and various energy and mineral resources in the Dongsheng area, Yimeng uplift. Oil and Gas Geology 27, 187–193 (in Chinese with English abstract).

Speight, J.G., 2006. The Chemistry and Technology of Petroleum, fourth ed. CRC Press, Taylor Francis Group, p. 984.

Sun, Y., 2005. A Study of Organic Geochemistry of the Dongsheng Uranium Deposit. Beijing Institute of Nuclear Geology, p. 66 (in Chinese).

Wang, W., Hou, G., Liu, F., Zhang, M., 2004. The hydrogeological characteristics of the Ordos Cretaceous artesian water basin and exploration problems. In: Hou, G., Zhang, M. (Eds.), Ground Water Resources and Their Sustainable Utilization in the Ordos Basin. Shaanxi Science and Technology Press, pp. 40–45 (in Chinese).

Wei, Y., Wang, Y., 2004. Comparison of enrichment patterns of various energy and mineral resources in the Ordos Basin. Oil & Gas Geology 25, 385–392 (in Chinese with English abstract).

Xia, Y., Lin, J., Liu, H., 2003. Geochronological studies of sandstone-type uranium deposits in major uranium-producing basins in northern China. Uranium Geology 19, 129–136 (in Chinese with English abstract).

Xiao, X., Li, Z., Chen, A., 2004. Evidence and significance of hydrothermal fluids in the formation of the Dongsheng sandstone-type uranium deposit. Mineralogy, Petrology and Geochemistry Letters 23, 301–304.

Xue, C.J., Chi, G.X., Xue, W., 2010. Interaction of two fluid systems in the formation of sandstone-hosted uranium deposits in the Ordos Basin: geochemical evidence and hydrodynamic modeling. Journal of Geochemical Exploration 106, 226–235.

Xue, W., Xue, C.J., Chi, G.X., Tu, Q., Kang, M., Gao, Y., 2009. Relationships between uranium mineralization and organic matter in Jurassic strata in the northeastern margin of the Ordos Basin. Geological Review 55, 361–369 (in Chinese with English abstract).

Yang, J.J., Pei, X.G., 1996. Geology of Natural Gas in China, Volume 4, the Ordos Basin. Petroleum Industry Press, Beijing, p. 108 (in Chinese).

Zhang, R., 2004. Relationships between deep gases and uranium mineralization in the Ordos Basin. Uranium Geology 20, 213–234 (in Chinese with English abstract).